Frequency and Clinical Implications of Fluid Dynamically Significant Diffuse Coronary Artery Disease Manifest as Graded, Longitudinal, Base-to-Apex Myocardial Perfusion Abnormalities by Noninvasive Positron Emission Tomography

K. Lance Gould, MD; Yuko Nakagawa, MD; Keiichi Nakagawa, MD; Stefano Sdringola, MD; Mary Jane Hess, RN; Mary Haynie, RN, MBA; Neal Parker, MS; Nizar Mullani, BS; Richard Kirkeeide, PhD

Background—Diffuse coronary atherosclerosis is the substrate for plaque rupture and coronary events. Therefore, in patients with mild arteriographic coronary artery disease without significant segmental dipyridamole-induced myocardial perfusion defects, we tested the hypothesis that fluid dynamically significant diffuse coronary artery narrowing is frequently manifest as a graded, longitudinal, base-to-apex myocardial perfusion abnormality by noninvasive PET.

Methods and Results—In this study, 1001 patients with documented coronary artery disease by coronary arteriography showing any visible coronary artery narrowing underwent rest-dipyridamole PET perfusion imaging. Quantitative severity of dipyridamole-induced, circumscribed, segmental PET perfusion defects was objectively measured by automated software as the minimum quadrant average relative activity indicating localized flow limiting stenoses. Quantitative severity of the graded, longitudinal, base-to-apex myocardial perfusion gradient indicating fluid dynamic effects of diffuse coronary artery narrowing was objectively measured by automated software as the spatial slope of relative activity along the cardiac longitudinal axis.

Conclusions—In patients with mild arteriographic disease without statistically significant dipyridamole-induced segmental myocardial perfusion defects caused by flow-limiting stenoses compared with normal control subjects, there was a graded, longitudinal, base-to-apex myocardial perfusion gradient significantly different from normal control subjects ($P=0.001$) that was also observed for moderate to severe dipyridamole-induced segmental perfusion defects ($P=0.0001$), indicating diffuse disease underlying segmental perfusion defects; 43% of patients with or without segmental perfusion defects demonstrated graded, longitudinal, base-to-apex perfusion abnormalities beyond ± 2 SD of normal control subjects, indicating diffuse coronary arterial narrowing by noninvasive PET perfusion imaging. **(*Circulation*. 2000;101:1931-1939.)**

Key Words: perfusion ■ coronary disease ■ tomography ■ atherosclerosis

Diffuse coronary artery disease without segmental stenosis is frequently the substrate for plaque rupture and coronary events.[1–3] However, the frequency and fluid dynamic severity of diffuse coronary artery narrowing in patients with coronary artery disease have not been previously described. In contrast to segmental, circumscribed perfusion defects caused by segmental coronary artery stenoses, diffuse coronary artery narrowing would be expected to cause graded, progressively decreasing perfusion along the base-to-apex, longitudinal axis of the heart after dipyridamole or adenosine stress, being best at the base of the heart, lower in middle sections, and lowest at the apex in a continuous graded change, as illustrated in Figure 1A.[4,5]

Accordingly, we hypothesized that in patients with mild arteriographic coronary artery disease without significant segmental perfusion defects, myocardial perfusion imaging by PET after dipyridamole would demonstrate fluid dynamic effects of diffuse narrowing as a decreasing perfusion gradient of relative activity from base to apex along the long axis of the left ventricle that was statistically significantly different from normal volunteers without coronary artery disease or risk factors.

Received March 11, 1999; revision received November 2, 1999; accepted November 19, 1999.

From the Weatherhead PET Center for Preventing and Reversing Atherosclerosis, (K.L.G., M.J.H., M.H., N.P.), University of Texas Medical School (S.S.), Houston; Memorial Hermann Health Care System and Hermann Hospital, Houston, Tex; and Chiba University, Chiba, Japan (Y.N., K.N.).

Guest Editor for this article was Heinrich R. Schelbert, MD, PhD, UCLA School of Medicine, Los Angeles, Calif.

Reprint requests to K. Lance Gould, MD, PET Imaging Center, University of Texas Medical School, Room 4.256 MSB, Houston, TX 77030.

Circulation **is available at http://www.circulationaha.org**

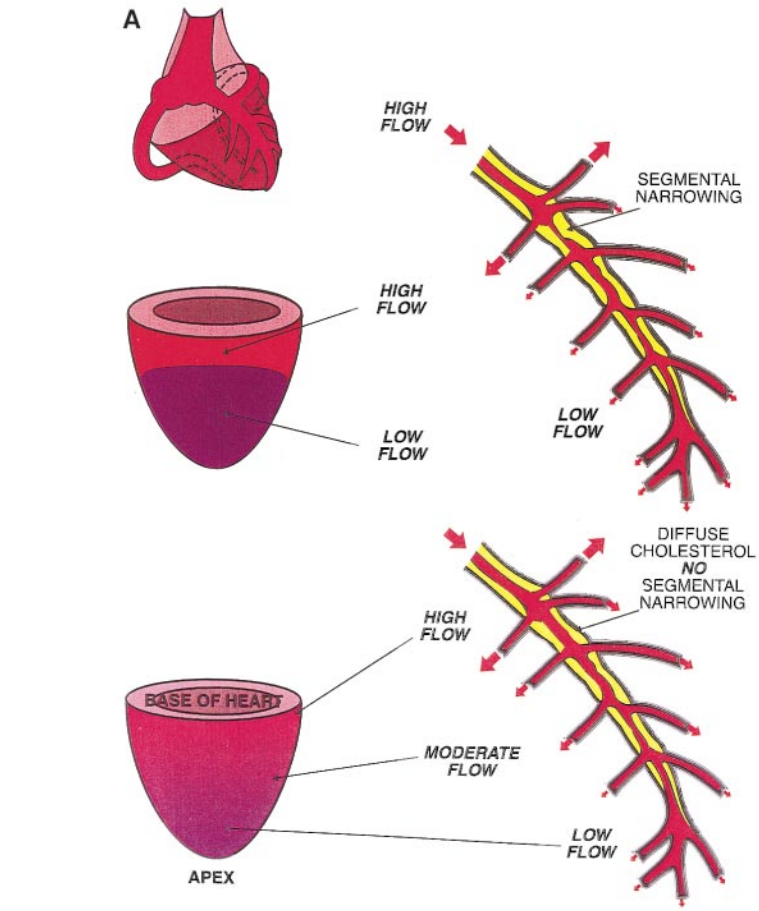

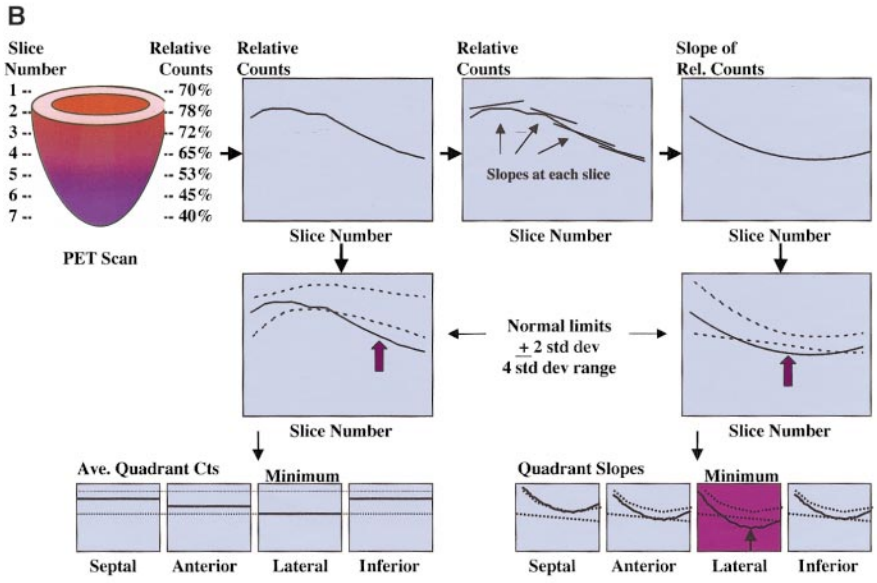

Figure 1. A, Longitudinal, base-to-apex myocardial perfusion abnormality caused by diffuse coronary artery narrowing compared with segmental perfusion defects caused by localized stenoses. B, Longitudinal analysis protocol. Purple arrows and purple box indicate abnormal longitudinal, base-to-apex distribution of relative activity outside 2 SD of normal control subjects in absence of segmental localized perfusion defect.

Methods

Study Subjects

After informed consent approved by the institutional review committee, 1001 men and women 30 to 88 years of age who were being clinically evaluated for coronary artery disease underwent myocardial PET perfusion imaging at rest and after dipyridamole with ^{13}N ammonia. Of these, 751 had coronary arteriography documenting coronary artery disease ranging from luminal irregularities or mild stenoses of only 10% diameter narrowing to complete occlusion by visual inspection. Because of the limitations of coronary arteriography for assessing combined diffuse and multisegmental coronary artery disease,[4–8] the arteriograms were used to define a group of patients with coronary atherosclerosis by the accepted standard of arteriography without controversies about its quantitative accuracy.

To assess "referral bias" of catheterized patients, 250 subjects were studied for coronary artery disease by rest dipyridamole PET without coronary arteriography. Seventeen normal volunteers 23 to

57 years of age without a history of smoking, a family history, hypercholesterolemia, hypertension, obesity, diabetes, or excessive alcohol or recreational drug use underwent rest dipyridamole PET imaging without arteriography.

On the basis of the automated quantitative analysis of PET perfusion images described, study subjects were categorized automatically into groups corresponding to normal, mild, moderate, and severe segmental perfusion defects on dipyridamole PET studies by automated, objectively measured, predefined computer criteria. Group 1 was made up of normal volunteers (n=17). Group 2 comprised patients with a severe regional segmental perfusion abnormality on the rest PET perfusion image (n=145) defined as ≥1 quadrant of the anterior, septal, lateral, and inferior quadrants of the 3-dimensional (3D) topographic cardiac display with an average quadrant activity that was ≤60% of the maximum in the heart. This group included patients with substantial myocardial scar or severe segmental perfusion defects by resting and dipyridamole PET. Group 3 was made up of patients with rest PET perfusion images having all quadrants of the 3D topographic display with activity >60% of the maximum and dipyridamole images with ≥1 quadrant activity <60% of maximum for the heart (n=125). This group included patients without significant myocardial scar but severe regional segmental dipyridamole-induced perfusion defects. Group 4 was patients with rest perfusion images having all quadrants of the 3D topographic display with activity >60% of maximum in the heart and dipyridamole images with ≥1 quadrant having activity 60% to 70% of the maximum in the heart (n=251). This group included patients without significant myocardial scar but with moderate regional segmental dipyridamole-induced perfusion defects. Group 5 was comprised of patients with rest perfusion images having all quadrants of the 3D topographic display with activity >60% of maximum in the heart and dipyridamole images with all quadrants having activity >70% of maximum in the heart (n=230). This group includes patients without significant myocardial scar but with mild segmental dipyridamole-induced perfusion defects or no stress-induced perfusion defects. Group 6 was patients who had a rest-dipyridamole PET perfusion study but did not have a coronary arteriogram (n=250). This group was analyzed in subcategories like groups 2 through 5 to demonstrate that there were no systematic differences in the PET perfusion studies in patients with or without an arteriogram as a result of referral bias.

PET Imaging

PET imaging of myocardial perfusion at rest and after dipyridamole was carried out as previously described.[5,9–11] Patients stopped smoking 4 hours before the PET study, fasted for 8 hours, and stopped intake of caffeine and theophylline for 24 hours before the PET study. PET was performed with the University of Texas–designed cesium fluoride, multislice tomograph with a reconstructed resolution of 12-mm full-width at half-maximum (FWHM) in plane and 14-mm FWHM axially. Transmission images containing 100 to 150 million counts were obtained to correct for photon attenuation with the segmented attenuation correction method first reported from this laboratory.[12] Emission images were obtained after injection of 18 mCi IV cyclotron-produced ^{13}N ammonia as previously described[9–11] and contained 20 to 40 million counts.

At 40 minutes after the first dose of ammonia, dipyridamole ($0.142\ mg \cdot kg^{-1} \cdot min^{-1}$) was infused for 4 minutes. Four minutes later, a second dose of ^{13}N ammonia was injected intravenously. PET imaging was repeated by the protocol used for the resting study. Aminophylline (125 mg IV) was given for angina.

Automated Quantitative Analysis of PET

Automated analysis of PET abnormalities was carried out without observer bias with previously described software.[5,9–11] A 3D restructuring algorithm generated short- and long-axis views from PET transaxial cardiac images perpendicular to and parallel to, respectively, the long axis of the left ventricle. To avoid the spatial distortion inherent in polar displays, circumferential profiles were used to reconstruct 3D topographic views of the left ventricle reflecting relative regional activity. The 3D topographic views were divided into fixed sections consisting of a septal, anterior, lateral and inferior quadrant as previously illustrated.[5,10,11] A mean algorithm determined, for each of the 3D topographic views, the mean activity level in each of these 4 regions expressed as relative activity levels normalized to the maximum 2% of pixels for the whole-heart data set for each of the 3D topographic views. Finally, an algorithm automatically identified regions of each topographic view that have values deviating outside ±2-SD limits of normal values (4-SD range) on the basis of 17 normal volunteers and computed the percent of circumferential profile units outside ±2-SD limits (4-SD range).

Analysis of the Relative Distribution of Activity Along the Long Axis of the Left Ventricle

The 3D restructuring algorithm generated 34 tomographic slices perpendicular to the long axis of the left ventricle labeled slice 1 at the base of the heart to slice 34 at the apex of the heart. Slices 1 through 7 and 30 through 34 were discarded as a result of count variability caused by the membranous septum, by variability in locating the last apical slice, and by partial volume errors resulting from small object size at the apex. For each slice 8 through 29, the average relative activity expressed as percent of maximum was determined for each slice in the septal, anterior, lateral, and inferior quadrants. The relative activity of each slice in each quadrant was plotted on the vertical axis for each slice 8 through 29 on the horizontal axis for each quadrant of the heart.

The distribution of activity from base (slice 8) to apex (slice 29) was then best fit to a third-degree polynomial, the first derivative of which was determined as the spatial slope or spatial rate of change in activity along the long axis of each quadrant. The relative activity for each slice and the slope value for each slice 8 to 29 were then also plotted on the vertical axis for slice number on the horizontal axis for each quadrant. Negative slope values indicate decreasing activity along the long axis of the left ventricle, and positive slope values indicate increasing values along the long axis of the left ventricle.

Rest and dipyridamole images were analyzed similarly for average relative uptake in each quadrant, for the longitudinal distribution of relative activity for each quadrant, and for the rate of change in activity or slope along the long axis of the left ventricle. Mean values and ±2-SD limits of relative activity and rate of change in relative activity along the long axis of the left ventricle (slope) were determined for each slice 8 to 29 for each quadrant for the 17 normal volunteers. The ±2-SD limits of this normal group were plotted for each slice as reference limits on the graphs of relative uptake and slope for each patient. The maximum rate of decrease in relative activity along the long axis of the left ventricle (maximum negative slope or minimum slope value including the sign) was determined for each quadrant of each patient.

PET End Points

The end points were the severity of perfusion defects on PET images and the slope or rate of change of relative activity along the long axis of the left ventricle after dipyridamole stress, all measured automatically. Severity was defined as the lowest quadrant average relative activity or the average relative activity for the quadrant having the lowest average activity of the anterior, septal, lateral, and inferior quadrants for each patient or normal volunteer. The quadrant with the lowest or minimum relative activity contained the perfusion defect(s). This end point quantifies the relative severity of segmental perfusion abnormalities at rest and after dipyridamole stress. In prior studies, this end point, lowest quadrant average activity, has been the most sensitive and reliable with the least statistical variability for distinguishing between groups of patients by PET perfusion imaging.[5,9–11]

The end point for the longitudinal distribution of activity was the minimum quadrant slope of radionuclide uptake for each patient, defined as the minimum value (maximum negative value) of the slope of the 4 quadrants. It was calculated as the first derivative of the third-power polynomial equation best fitting the longitudinal distribution of relative activity for slices 8 through 29 of each of the

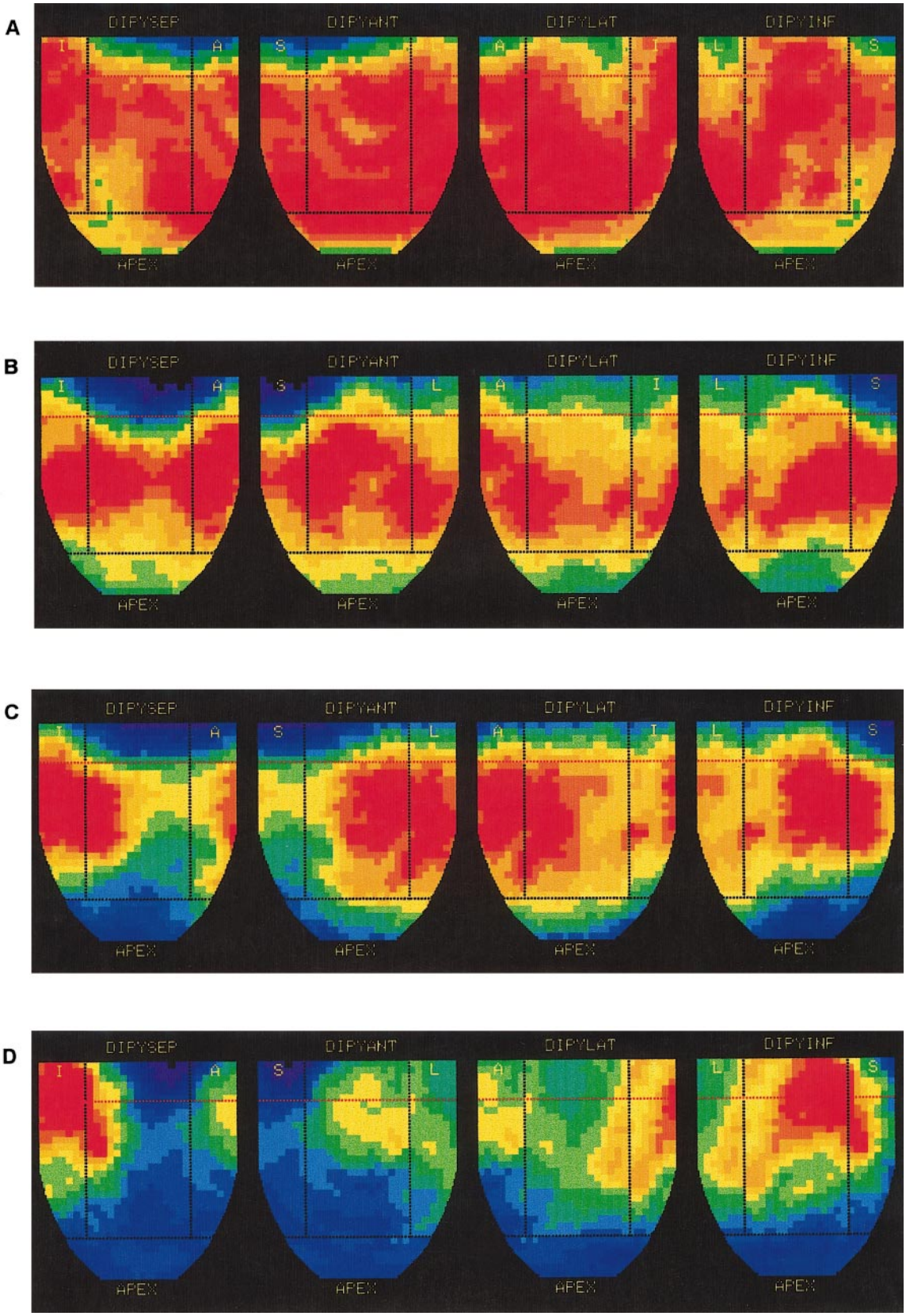

Figure 2. A, Normal myocardial perfusion by PET after dipyridamole. B, Mild longitudinal, base-to-apex myocardial perfusion abnormality after dipyridamole in patient with normal resting PET scan. C, Moderate longitudinal, base-to-apex myocardial perfusion abnormality after dipyridamole in different patient, also with normal resting scan. D, Severe longitudinal, base-to-apex myocardial perfusion abnormality after dipyridamole in different patient, also with normal resting PET scan. Views are left to right septal, anterior, lateral, and inferior. Color scale of relative myocardial activity indicating myocardial perfusion is red for maximum (100%) downward in 5% increments through yellow, green, blue, and black indicating minimum activity.

4 quadrants for each patient after dipyridamole. The units of the slope values were change in relative activity per slice for each slice from base to apex. The minimum slope or maximum negative slope of the 4 quadrants was a single number that quantifies the fluid dynamic effects of diffuse coronary narrowing in the distribution of any single coronary artery in a single patient. The 2 independently determined end points allowed statistical comparisons: 1 end point reflected regional flow-limiting stenoses, and the other reflected diffuse coronary artery narrowing. Figure 1B illustrates the analysis protocol and how the longitudinal base-to-apex perfusion gradient may be abnormal (purple arrows and purple box) in the absence of a localized segmental perfusion defect.

Statistical Analysis

Automated measures of differences in these end points between groups of patients were analyzed as continuous variables by use of ANOVA with the Bonferroni-Dunn post hoc correction in Statview software.[13–15] Data in the Table are reported as mean±SD. For discrete variables such as number or percent of subjects showing changes outside ±2 SD of normal control subjects, the significance of differences between groups was determined by McNemar's test.[15]

Results

Figure 2A illustrates a normal myocardial perfusion image by PET after dipyridamole. Figure 2B through 2D illustrates progressively more severe, graded, longitudinal, base-to-apex perfusion gradients after dipyridamole stress from different patients with normal resting scans.

Figure 3 illustrates progressive abnormalities of the quadrant relative activity plotted for the most affected quadrant for examples in Figure 2B through 2D. Figure 3A corresponds to Figure 2B; it shows a mild, longitudinal, base-to-apex perfusion gradient corresponding to the mild visual gradient in Figure 2B. Figure 3B shows a moderate, longitudinal, base-to-apex gradient corresponding to Figure 2C. Figure 3C shows a severe, longitudinal, base-to-apex perfusion gradient corresponding to Figure 2D. Dashed lines show ±2 SD of normal control subjects (a 4-SD range).

Figure 4 shows the slope of decreasing activity along the long axis of the left ventricle for the same quadrant of Figure 2B through 2D. Dashed lines show ±2 SD of normal control subjects. The minimum slopes are outside these normal limits for these 3 examples of progressively severe, longitudinal, base-to-apex myocardial perfusion gradients.

Longitudinal Perfusion Gradient and Severity of Coronary Artery Disease

The analysis illustrated in the 3 examples of Figures 3 and 4 was carried out for 1001 patients categorized into the 6 groups defined in the Methods section: normal control subjects (group 1); those with severe resting perfusion abnormalities (group 2), severe perfusion abnormalities after dipyridamole but not at rest (group 3), moderate dipyridamole-induced abnormalities but not at rest (group 4), and mild dipyridamole-induced abnormalities but not at rest (group 5); and patients without an arteriogram (group 6). The lowest quadrant average relative activity and minimum quadrant slope were determined for each patient in these groups. The mean values of the lowest quadrant average relative activity and minimum quadrant slope were calculated for each group and compared with these same end points in the normal group by 2-tailed, unpaired *t* testing (Bonferroni-Dunn) with results

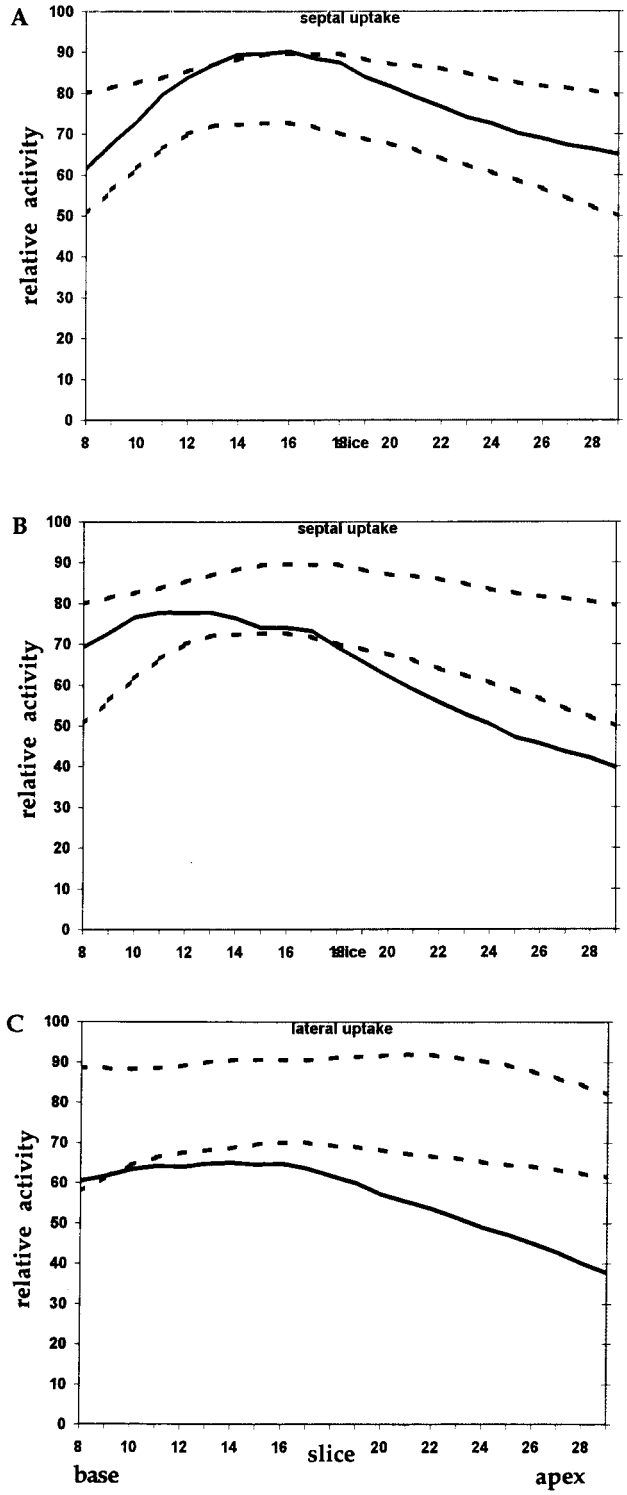

Figure 3. Relative myocardial activity after dipyridamole on vertical axis for location along longitudinal axis of left ventricle on horizontal axis for most abnormal quadrant of 4 views for examples in Figure 2. A, Graph corresponds to Figure 2B and is normal although slope is abnormal as shown in next figure. B, Graph corresponds to Figure 2C. D, Graph corresponds to Figure 2D. Light dashed lines indicate ±2 SD of normal control subjects.

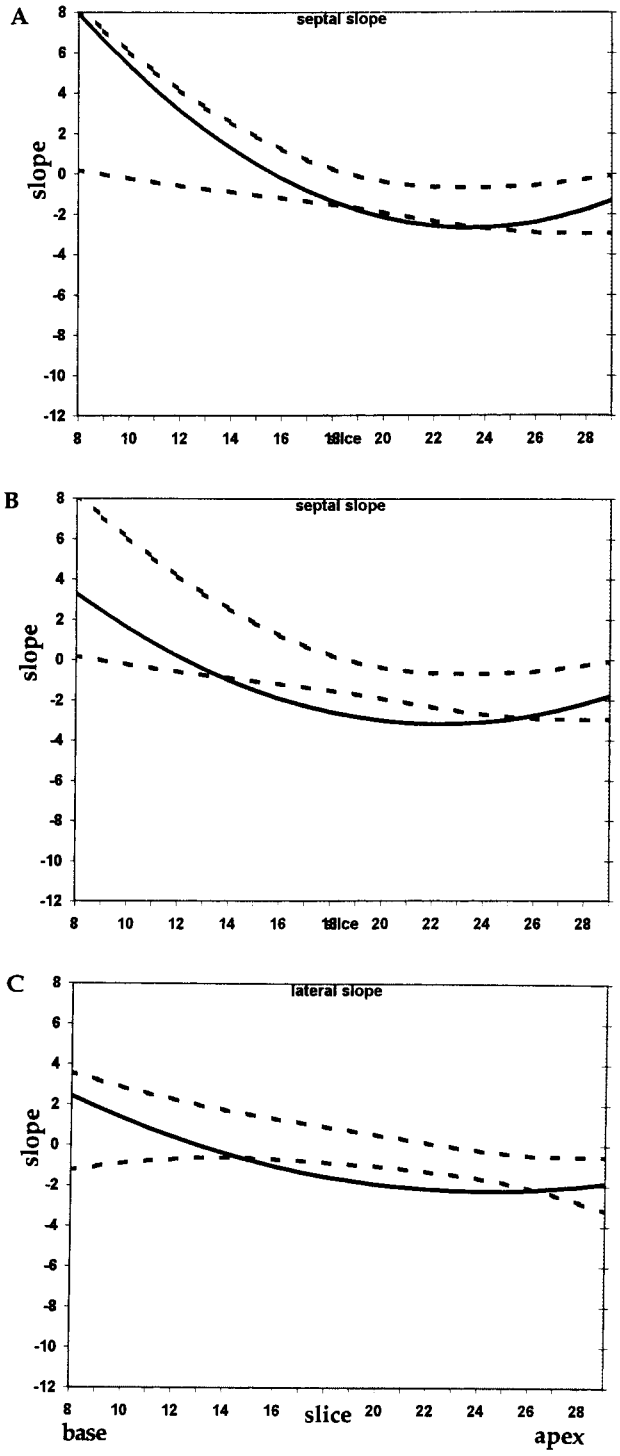

Figure 4. Slopes of polynomial best fitting relative uptake along longitudinal axis on vertical axis for each slice from base (slice 8) to apex (slice 29) on horizontal axis for most abnormal quadrant of 4 views in examples in Figure 2. A, Graph corresponds to Figure 2B; B, graph corresponds to Figure 2C; C, graph corresponds to Figure 2D. Light dashed lines indicate ±2 SD of normal control subjects. Minimum slope or maximal negative value is single number characterizing effects of diffuse disease for that quadrant or heart. Minimum slope values are outside ±2-SD limits for all 3 examples of mildly, moderately, and severely abnormal longitudinal perfusion gradients.

shown in Figure 5. For patients with severe perfusion defects, groups 2 and 3, the quadrant with minimum slope commonly corresponded to that with lowest quadrant average relative activity although other quadrants also had abnormal slopes. For patients with mild to moderate perfusion defects, the quadrant with minimum slope commonly did not correspond to that with lowest average activity.

Patients with documented coronary artery disease and only moderate (group 4) to mild (groups 5 and 6) segmental perfusion abnormalities after dipyridamole that were not statistically significantly worse than normal control subjects had graded base-to-apex, longitudinal myocardial perfusion gradients on dipyridamole images with minimum quadrant slopes that were significantly different from normal control subjects ($P=0.001$ to 0.005). It is important to emphasize that the severity of segmental perfusion defects quantified as the minimum quadrant average relative activity for group 5 and 6 were not significantly worse than the normal group. Thus, in mild to moderate coronary artery disease without quantitatively significant segmental perfusion defects caused by flow-limiting stenoses, there are quantitatively significant, graded, longitudinal, base-to-apex perfusion abnormalities with minimum quadrant slopes that are significantly worse than normal control subjects because of diffuse coronary artery disease.

Analysis of patients in group 6 subcategorized by the same criteria for groups 2 through 5 showed similar mean values of the lowest quadrant average relative uptake and minimum quadrant slope, suggesting no selection or referral bias in groups 2 through 5 who underwent coronary arteriography.

The Table shows the percent of patients in each group with lowest quadrant average relative activity or minimum quadrant slope outside ±2 SD of normal control subjects in ≥1 of the 4 quadrants of the dipyridamole PET study for each patient. In each group, 41% to 52% had a minimum quadrant slope outside ±2 SD of normal control subjects, associated in groups 2 and 3 with a significantly higher proportion of patients having severe resting perfusion defects caused by prior myocardial infarction (group 2) or severe dipyridamole-induced defects (group 3).

Some segmental perfusion defects were so severe that they obliterated the more subtle longitudinal, base-to-apex perfusion gradient. Consequently, the percent of patients with minimum slope outside normal limits for groups 2 and 3 with severe segmental PET perfusion abnormalities was significantly less than the percent of patients with significantly abnormal segmental perfusion defects. For patients in groups 4 through 6 with only mild to moderate segmental perfusion abnormalities, the percent of patients with significantly abnormal slope values was significantly larger than the percent of patients with significantly abnormal regional perfusion defects. For all 1001 patients, 443 (44.3%) had a minimum slope of longitudinal relative activity outside ±2 SD of normal control subjects.

For patients with only mild to moderate segmental perfusion defects that were not quantitatively or significantly outside normal ±2 SD of normal control subjects, the minimum quadrant slope was frequently outside normal limits for individual patients. For the 533 patients with no

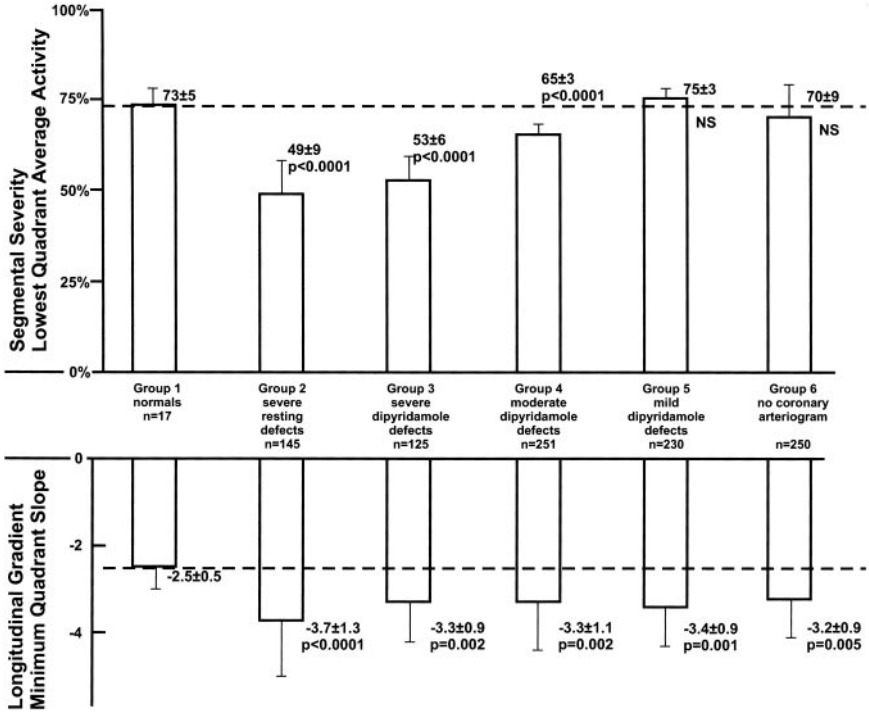

Figure 5. Mean values of lowest quadrant average relative activity and minimum quadrant slope for patients in each group. Dashed lines indicate mean values for normal control subjects. Probability values are for each group compared with normal control subjects by ANOVA with the Bonferroni-Dunn post hoc correction.

statistically significant, segmental perfusion defects outside normal limits caused by flow-limiting stenoses, 233 (43.7%) had a significantly abnormal, longitudinal, base-to-apex perfusion gradient outside ±2 SD of normal control subjects, indicating diffuse coronary artery disease without significant segmental flow-limiting stenoses.

Discussion

This study verifies for the first time in a large study population the hypothesis of widely prevalent, significant fluid dynamic effects of diffuse coronary artery disease manifest as a graded, longitudinal, base-to-apex myocardial perfusion gradient by cardiac PET perfusion imaging after dipyridamole stress as a noninvasive marker of diffuse coronary artery disease not observed in normal volunteers. It is commonly present and quantitatively severe enough to be outside ±2 SD of normal control subjects before regional segmental perfusion abnormalities become severe enough to fall outside the normal limits.

Clinical Implications

The gradual base-to-apex, longitudinal perfusion gradient observed on PET images is consistent with the observation that coronary flow reserve measured distally by intracoronary Doppler or pressure guide wires is lower than that measured proximally and correlates better with stress perfusion defects than proximal measurements of coronary flow reserve.[16–21] Thus, these PET findings correspond to flow velocity observations and provide a sound fluid dynamic basis for making flow velocity and pressure measurements by intracoronary wires along the entire length of a coronary artery as a pullback tracing from the most distal to proximal aspect of a coronary artery.[5]

Although we have used automated, objective measurements to demonstrate the concept without the imprecision or bias of observer interpretation, the longitudinal, base-to-apex perfusion gradient on the dipyridamole PET images is visually useful clinically after modest experience. It is useful mainly for identifying diffuse coronary artery narrowing in

Percentage of Patients With Severity of Segmental Perfusion Defects or Longitudinal Base-to-Apex Perfusion Gradient Outside 95% Confidence Limits of Normals

Category of Patients	No. Patients in Each Group	No. (%) of Patients With 1 Quadrant Outside 95% CI		
		Lowest Quadrant Average Activity (Segmental Perfusion Defect)		Minimum Quadrant Slope (Longitudinal Gradient)
Group 2, severe resting abnormality by PET perfusion imaging	145	143 (99)	$P<0.0000$	72 (50)
Group 3, severe segmental abnormality by dipyridamole PET	125	125 (100)	$P<0.0000$	65 (52)
Group 4, moderate segmental abnormality by dipyridamole PET	251	129 (51)	P=NS	102 (41)
Group 5, mild segmental abnormality by dipyridamole PET	230	4 (2)	$P<0.0000$	101 (44)
Group 6, no coronary arteriogram and dipyridamole PET	250	67 (27)	$P=0.0001$	103 (41)

P=significance by McNemar's test. 95% CI indicates 95% confidence intervals of normals.

the absence of flow-limiting stenoses that cause no regional perfusion defects.

Coronary arteriography has been the basis for definitive diagnosis and follow-up of changes in severity of disease but fails to detect most diffuse coronary atherosclerosis.[4–8] Furthermore, reliance on an invasive diagnostic test for lifelong, noninvasive lipid lowering precludes consideration of a principally noninvasive basis for identifying diffuse disease for vigorous cholesterol lowering.[5,22]

Study Limitations

In normal volunteers, there is a mild decrease in activity toward the apex of the heart most likely caused by partial volume loss associated with small object size of the cardiac apex relative to the spatial resolution of the PET scanner. We did not correct for partial volume errors because such corrections require assumptions that are questionable. The partial volume error in this study was addressed by comparing all patients to the ±2 SD of normal volunteers because partial volume errors apply equally to all groups of patients studied with same PET scanner and software. Unrecognized diffuse coronary artery disease in the normal subjects would tend to reduce the significance of differences between patients and normal control subjects.

Percent diameter stenosis on coronary arteriograms is commonly misleading, misinterpreted, or simply incorrect for assessing severity of coronary artery disease. Errors include estimated percent diameter narrowing, extensive disease in the supposed normal reference segment by intravascular ultrasound so that relative percent narrowing is essentially meaningless,[4–8] errors of 50% to 80% for coronary arteriography in identifying diffuse coronary artery disease,[6–8] and failure of arteriography to account for the hemodynamic effects of multiple stenoses or mixed segmental and diffuse disease.[5] The poor correlation between percent diameter stenosis and coronary flow reserve in multivessel disease has been well documented, making it a poor "gold standard" of severity. It does not need reiteration here.

Absolute perfusion was not determined in this study because relative distribution of radionuclide uptake along the long cardiac axis does not depend on knowledge of absolute perfusion and/or arterial input function. For diffuse disease affecting secondary coronary branches relatively uniformly, there would be no branch steal and therefore no longitudinal, base-to-apex perfusion gradient. Under these circumstances, absolute myocardial perfusion and perfusion reserve identify and quantify diffuse coronary artery disease in the absence of localized arteriographic stenoses.[23–25]

Early diffuse coronary atherosclerosis developing in large epicardial coronary arteries before secondary branches are affected may cause a longitudinal, base-to-apex perfusion gradient before coronary flow reserve is reduced. Late severe diffuse coronary atherosclerosis of large epicardial coronary arteries and secondary branches will reduce absolute coronary flow reserve without a longitudinal, base-to-apex perfusion gradient. Finally, some secondary coronary artery branches may terminate close to the AV ring instead of toward the cardiac apex. This anatomy may cause a basal defect, a reverse apex-to-base perfusion gradient, or a "double defect" at the base and apex separated by a zone of greater activity, particularly on the inferior wall because of codominant left circumflex and right coronary arteries.[5]

Conclusions

Myocardial perfusion imaging by PET after dipyridamole stress frequently demonstrates significant fluid dynamic effects of diffuse coronary artery disease manifest by a graded, longitudinal, base-to-apex perfusion abnormality not present in normal volunteers that may be useful clinically for identifying patients with coronary atherosclerosis in the absence of flow-limiting stenosis as the basis for vigorous secondary intervention with cholesterol-lowering drugs and risk factor modification. The present study reports a new fundamental observation in perfusion imaging in a large group of patients. However, extended clinical application of these observations requires further study.

Acknowledgments

Supported in part by NIH grant R0-1-HL-48574, the Weatherhead Endowment, and the Memorial Hermann Foundation.

References

1. Falk E, Shah PK, Fuster V. Coronary plaque disruption. *Circulation*. 1995;92:657–671.
2. Libby P. Molecular bases of the acute coronary syndromes. *Circulation*. 1995;91:2844–2850.
3. Farb A, Tang AL, Burke AP, Sessums L, Liang Y, Virmani R. Sudden coronary death: frequency of active coronary lesions, inactive coronary lesions, and myocardial infarction. *Circulation*. 1995;92:1701–1709.
4. Seiler C, Kirkeeide RL, Gould KL. Basic structure-function of the epicardial coronary vascular tree: the basis of quantitative coronary arteriography for diffuse coronary artery disease. *Circulation*,. 1992;85: 1987–2003.
5. Gould KL. *Coronary Artery Stenosis and Reversing Atherosclerosis*. 2nd ed. Arnold Publishing: New York: Oxford University Press; 1999.
6. Mintz GS, Painter JA, Pichard AD, Kent KM, Satler LF, Popma JJ, Chuang YC, Bucher TA, Sokolowicz LE, Leon MB. Atherosclerosis in angiographically "normal" coronary artery reference segments: an intravascular ultrasound study with clinical correlations. *J Am Coll Cardiol*. 1995;25:1479–1485.
7. Hausmann D, Johnson JA, Sudhir K, Mullen WL, Friedrich G, Fitzgerald PJ, Chou TM, Ports TA, Kane JP, Mallow MJ, Yock PG. Angiographically silent atherosclerosis detected in intravascular ultrasound in patients with familial hypercholesterolemia and familial combined hyperlipidemia: correlation with high density lipoproteins. *J Am Coll Cardiol*. 1996;27:1562–1570.
8. St Goar FG, Pinto JF, Alderman E, Fitzgerald PJ, Stinson EB, Billingham ME, Path FRC, Popp RL. Detection of coronary atherosclerosis in young adult hearts using intravascular ultrasound. *Circulation*. 1992;86:756–763.
9. Demer LL, Gould KL, Goldstein RA, Kirkeeide RL. Diagnosis of coronary artery disease by positron emission tomography: comparison to quantitative coronary arteriography in 193 patients. *Circulation*. 1989;79: 825–835.
10. Gould KL, Martucci JP, Goldberg DI, Hess MJ, Edens RP, Latifi R, Dudrick SJ. Short-term cholesterol lowering decreases in size and severity of perfusion abnormalities by positron emission tomography after dipyridamole in patients with coronary artery disease. *Circulation*. 1994;89:1530–1538.
11. Gould K, Ornish D, Scherwitz L, Brown S, Edens RP, Hess MJ, Mullani N, Bolomey L, Dobbs F, Armstrong WT, Merritt T, Ports T, Sparler S, Billings J. Changes in myocardial perfusion abnormalities by positron emission tomography after long-term, intense risk factor modification. *JAMA*. 1995;274:894–901.
12. Xu EZ, Mullani NA, Gould KL, Anderson WL. A segmented attenuation correction for PET. *J Nucl Med*. 1991;32:161–165.
13. Snedecor GW, Cochran WG. *Statistical Methods*. 8th ed. Ames, Iowa: Iowa State University Press; 1989.
14. *Stat View*. Berkeley, Calif: Abacus Concepts, Inc; 1992.

15. Armitage P. *Statistical Methods in Medical Research*. Oxford, UK: Black Scientific Publications; 1971.
16. Kern MJ, Anderson HV. A symposium: the clinical applications of the intracoronary Doppler guidewire flow velocity in patients: understanding blood flow beyond the coronary stenosis. *Am J Cardiol*. 1993;71: 1D–70D.
17. Kern MJ, Donohue TJ, Aguirre FV, Bach RG, Caracciolo EA, Ofili E, Labovitz AJ. Assessment of angiographically intermediate coronary artery stenosis using the Doppler flowwire. *Am J Cardiol*. 1993;71: 26D–33D.
18. Donohue TJ, Miller DD, Bach RG, Tron C, Wolford T, Caracciolo EA, Aguirre FV, Younis LT, Chaitman BR, Kern MJ. Correlation of poststenotic hyperemic coronary flow velocity and pressure with abnormal stress myocardial perfusion imaging in coronary artery disease. *Am J Cardiol*. 1996;77:948–954.
19. Pijls NHJ, Van Gelder B, Van der Voort P, Peels K, Bracke FALE, Bonier HJRM, El Gamal MIH. Fractional flow reserve: a useful index to evaluate the influence of an epicardial coronary stenosis on myocardial blood flow. *Circulation*. 1995;92:3183–3193.
20. Pijls NHJ, de Bruyne B, Peels K, van der Voort PH, Bonnier HJRM, Bartunek J, Koolen JJ. Measurement of fractional flow reserve to assess the functional severity of coronary artery stenoses. *N Engl J Med*. 1996; 334:1703–1708.
21. De Bruyne B, Bartunek J, Sys S, Heyndrickx GR. Relation between myocardial fractional flow reserve calculated from coronary pressure measurements and exercise-induced myocardial ischemia. *Circulation*. 1995;92:39–46.
22. Gould KL. *Heal Your Heart: How To Prevent or Reverse Your Heart Disease*. New Brunswick, NJ: Rutgers University Press; 1998.
23. Uren NG, Marraccini P, Gistri R, de Silva R, Camici PG. Altered coronary vasodilator reserve and metabolism in myocardium subtended by normal arteries in patients with coronary artery disease. *J Am Coll Cardiol*. 1993;22:650–658.
24. Di Carli M, Czernin J, Hoh LK, Gerbando VH, Brunken RL, Huang SC, Phelps ME, Schelbert HR. Relation among stenosis severity, myocardial blood flow, and flow reserve in patients with coronary artery disease. *Circulation*. 1995;91:1944–1951.
25. Beanlands RSB, Musik O, Melon P, Sutor R, Sawada S, Muller D, Bordie D, Hutchins GO, Schwaiger M. Non-invasive quantification of regional myocardial flow reserve in patients with coronary atherosclerosis using N-13 ammonia positron emission tomography. *J Am Coll Cardiol*. 1995; 26:1465–1475.